of practical enolate chemistry. In accord with this analysis, treatment of (*R*)-(+)-verbenone[10] with KO-*t*-Bu in DME at 0 °C followed by addition of dibromide **5**,[12] which for the purposes of this study serves as a *representative* C ring precursor,[13] yielded the C11 alkylated product **6** (50–60%).[14] Subsequent reorganization of the pinene nucleus of **6**, requiring a 1,3-alkyl shift of C15 from C13 to C11, was inspired by the pioneering photochemical studies on the conversion of verbenone to chrysanthenone.[15] With the alkylated verbenone **6**, this photoinduced shift occurred quickly and efficiently (degassed cyclohexane/Hanovia/Pyrex/20 min), providing the desired rearrangement product **7** in 85% isolated yield.

The next stage of our plan, involving the addition of C3 to the carbonyl group of **7**, was designed to exploit the relative ease of intramolecularly forming a six-membered ring, which as a consequence of its fusion to a strained four-membered ring was expected to fragment to the eight-membered B ring of the taxanes. In accord with this plan, tetracyclic alcohol **8** was formed in 67% yield when bromide **7** was treated with *t*-BuLi. It is noteworthy that while the aryllithium intermediate in this process adds readily to the C2 carbonyl the more reactive *t*-BuLi does not, owing in part to steric congestion at C2 and the facility of lithium–halogen exchange. Epoxidation of alcohol **8** using $\mathrm{Ti(O\text{-}\mathit{i}\text{-}Pr)_4}$/*t*-BuOOH at 0 °C resulted in the completely stereocontrolled formation of the epoxide **9** in 60–70% yield, thereby setting the necessary stereochemistry at C13 for eventual attachment of taxol-like side chains. Due to the lability of this epoxide, it was directly treated with DABCO to effect fragmentation to the desired tricycle **10a** in 80% yield.[16] In analogy with the observations of Shea and co-workers,[17] tricycle **10a** exists at 25 °C as a 9:1 mixture of two slowly interconverting atropoisomers.

At this point all that remained to complete the A ring functionality required for taxol was incorporation of the bridgehead hydroxyl group at C1. While oxygenation of a bridgehead enolate represented a potentially practical solution to this goal, computer modeling indicated that only in the minor atropoisomer of **10a** is the C1 hydrogen suitably aligned for enolate formation. However, at higher temperatures (60 °C) where isomer interconversion is rapid, complete hydrogen–deuterium exchange at C1 was expected and indeed observed when the ether derivative **10b** was treated with $\mathrm{NaOCD_3}$ in $\mathrm{CD_3OD}$. Moreover, when this ether (**10b**) was treated with KO-*t*-Bu in THF at 60 °C in the presence of DMSO and $\mathrm{O_2}$ gas for 30 min, formation of the desired bridgehead hydroxyl product **11** was accomplished in 80% isolated yield. The final task in converting all 10 carbons of pinene to the corresponding functionalized carbons of the taxol nucleus was achieved through thermodynamically controlled reduction of **11** ($\mathrm{Na/EtOH/Et_2O}$/0 °C), affording diol **12** in 60% yield.[18]

In summary, a new and versatile strategy has been described that offers promise for the synthesis of taxol and is currently being used for the practical formation of taxol analogues[19] as required for molecular mode of action and drug development studies. In the current example, the tricyclic core of the taxanes is assembled with enantiomeric control in five steps from pinene and further elaborated to produce the complete functionality and stereochemistry of the taxol A ring and strategically located and differentiated functionality at other key sites in three additional steps. This sequence is sufficiently straightforward to be conducted on a large scale; current runs have started with 1–2 mol but could be readily increased. More generally, this process demonstrates how the 10 carbons of pinene can be incorporated into the 20-carbon taxol core with control of absolute and relative stereochemistry and substitution. Moreover, this chemistry can be extended to widely varied and functionalized aromatic and nonaromatic C ring precursors. These studies will be reported in due course.

Acknowledgment. This research was supported by grants from the National Institutes of Health (CA31845) and Bristol-Myers Squibb. T.P.M. is grateful to the National Science Foundation for predoctoral fellowship support in the first phase of this work in 1989. The authors are especially indebted to Drs. S. Broder, B. Chabner, and M. Suffness of the NIH and Dr. T. Doyle of BMS for invaluable discussions on taxol clinical and supply studies.

Supplementary Material Available: Listings of ^{1}H NMR, ^{13}C NMR, FTIR, and high-resolution mass spectroscopic and/or elemental analysis data for **6–8**, **10a**,**b**, **11**, and **12** (5 pages). Ordering information is given on any current masthead page.

---

(12) Compound **5** was prepared on a multimole scale in two steps from methyl 2-bromobenzoate (i. MeMgBr addition at 0 °C, followed by distillative dehydration of the carbinol product over $\mathrm{KHSO_4}$ (93%) (see Fleming, I.; Woolias, M. *J. Chem. Soc., Perkin Trans. 1* **1979**, 829). ii. Allylic bromination with $\mathrm{NBS/(PhCOO)_2}$) (83%)).

(13) This reaction has been conducted on a multimole scale. We have also achieved related alkylations of verbenone with a wide range of aromatic and nonaromatic C ring precursors. Methods for condensation with aldehydes and esters have also been developed. T. Glass, T. Mucciaro, T. Ohkuma, B. Peschke, A. Shuker, J. Sutton, L. Wessjohann, Stanford University, unpublished results, 1989 to the present.

(14) All new compounds were characterized by ^{1}H NMR, ^{13}C NMR, FTIR, and HRMS or elemental analysis.

(15) (a) Hurst, J. J.; Whitham, G. H. *J. Chem. Soc.* **1960**, 2864. (b) Erman, W. F. *J. Am. Chem. Soc.* **1967**, *89*, 3828.

(16) The structure of the TBS ether (**10b**) has been confirmed by an X-ray crystal structure determination performed by Dr. Qi Gao of Bristol-Myers Squibb. Details will be provided in a separate publication.

(17) Shea, K. J.; Gilman, J. W.; Haffner, C. D.; Dougherty, T. K. *J. Am. Chem. Soc.* **1986**, *108*, 4953.

(18) Reduction of **11** with LAH (ether, 0 °C) provided the C2 epimer of **12** (92%). The stereochemical assignments are fully in accord with theoretical expectations and supported by side-by-side comparisons of anisotropic shifting of the methyl groups observed in the NMR spectra of the acetonides of **12** and of its C2 epimer.

(19) Jim Sutton, Stanford University, unpublished results, 1991. The side chain was synthesized by the method of Denis et al. (Denis, J.-N.; Correa, A.; Greene, A. E. *J. Org. Chem.* **1990**, *55*, 1957) and attached by the method of Swindell et al. (Swindell, C. S.; Krauss, N. E.; Horwitz, S. B.; Ringel, I. *J. Med. Chem.* **1991**, *34*, 1176).

CASSCF Calculations Find That a D_{8h} Geometry Is the Transition State for Double-Bond Shifting in Cyclooctatetraene

David A. Hrovat and Weston Thatcher Borden*

Department of Chemistry
University of Washington
Seattle, Washington 98195

Received March 13, 1992

NMR studies have found that in cyclooctatetraene (COT)[1] the barrier to double-bond shifting is approximately 14 kcal/mol.[2,3b] Additional dynamic NMR experiments on monosubstituted derivatives of COT found the barrier to bond shifting to be 3–4 kcal/mol higher than the barrier to ring inversion.[3,4] With the assumption that the transition states for both processes have planar geometries, the difference in barrier heights represents the energy required to delocalize the double bonds in going from the D_{4h} transition state for ring inversion to the D_{8h} transition state for bond shifting (Figure 1).[3]

The assumption that bond shifting in COT requires a planar ring has recently been questioned.[5,6] Paquette and co-workers[5]

---

(1) Reviews: Paquette, L. A. *Tetrahedron* **1975**, *31*, 2855. Fray, G. I.; Saxton, R. G. The *Chemistry of Cyclooctatetraene and Its Derivatives*; Cambridge University Press: New York, 1978.

(2) Anet, F. A. L. *J. Am. Chem. Soc.* **1962**, *84*, 671. Slightly lower values have been reported for COT in liquid crystals (Naor, R.; Luz, Z. *J. Chem. Phys.* **1982**, *76*, 5662) and for fluoro-COT (Gwynn, D. E.; Whitesides, G. M.; Roberts, J. D. *J. Am. Chem. Soc.* **1965**, *87*, 2862).

(3) (a) Anet, F. A. L.; Bourn, A. J.; Lin, Y. S. *J. Am. Chem. Soc.* **1964**, *86*, 3576. (b) Oth, J. F. M. *Pure Appl. Chem.* **1971**, *25*, 573.

(4) Steric effects in substituted COTs tend to increase the barrier heights for both bond shifting and ring inversion and in multiply substituted COT derivatives steric effects also reduce the difference between the two barrier heights. Review: Paquette, L. A. *Pure Appl. Chem.* **1982**, *54*, 987.

0002-7863/92/1514-5879$03.00/0 © 1992 American Chemical Society

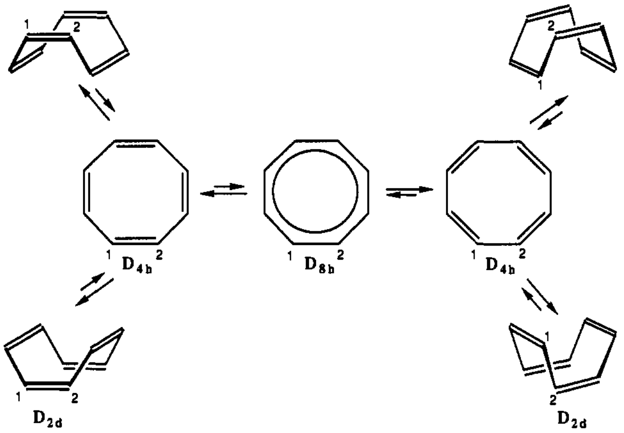

Figure 1. Schematic depiction of ring inversion and bond shifting in D_{2d} COT via, respectively, D_{4h} and D_{8h} transition states. A molecule crossing the D_{8h} transition state need not necessarily pass through a D_{4h} geometry.

have interpreted their studies of bond shifting in 1,*n*-annulated derivatives of COT in terms of a flattened, saddle-shaped, transition state geometry of the type proposed by Ermer and coworkers.[6] Ermer has argued that a D_{8h} geometry for COT is likely to have three negative force constants: one for going to bond-alternated, D_{4h} geometries via a mode of B_{1g} symmetry and two for going to tub-shaped D_{2d} minima and flattened saddle-shaped D_{2d} transition states via degenerate modes of E_{2u} symmetry.

However, the force constants for E_{2u} ring puckering need not necessarily be negative in D_{8h} COT. A planar D_{4h} transition state for COT inversion must have exactly one negative force constant for ring puckering. The negative force constant corresponds to torsions about single, not double, C–C bonds. As shown in Figure 1, in going from one bond-alternated, D_{4h} geometry to the other, as the double bonds shift, the two different force constants for torsions about C–C bonds between different atoms (e.g., C_1–C_2 and C_2–C_3) must each change sign. Since the force constants for ring puckering in planar COT each change sign along the coordinate for bond shifting, at the D_{8h} geometry, where symmetry requires that the two force constants for torsions about the partial C–C double bonds must be identical, these degenerate, E_{2u} force constants could both be either positive or negative.

As Ermer notes, "With a good quantum mechanical model, the calculation and diagonalization of the force constant matrices of the...stationary point conformations of [COT] would be highly desirable in order to gain further quantitative insight into the inversion and bond shift mechanisms."[6] We have performed such calculations, using MCSCF wave functions that contain configurations corresponding to all possible occupancies of eight orbitals by the eight electrons that are "active" in bond shifting. These complete active space (CAS) SCF calculations, with both the 3-21G[7] and 6-31G*[8] basis sets, find that bond shifting in COT occurs via a planar transition state of D_{8h} symmetry.

D_{2d}, D_{4h}, and D_{8h} geometries were optimized[9] and vibrational analyses performed with CASSCF/3-21G calculations.[10] The vibrational analyses revealed the tub-shaped D_{2d} geometry to be an energy minimum and the planar D_{4h} and D_{8h} geometries both to be transition states.

Table I. Absolute (hartrees) and Relative (kcal/mol) CASSCF Energies Computed for CASSCF/3-21G Optimized D_{2d}, D_{4h}, and D_{8h} Geometries of Singlet COT, Including Corrections for Differences in CASSCF/3-21G Zero-Point Energies (ΔZPE)

calculation	D_{2d}	D_{4h}	D_{8h}
3-21G	−305.9237	13.2	18.3[a]
3-21G + ΔZPE	0	13.8	16.6
6-31G*	−307.6350	10.0	16.4[b,c]
6-31G* + ΔZPE	0	10.6	14.7

[a] At the CASSCF/3-21G optimized D_{8h} geometry for the singlet, the lowest triplet lies 17.4 kcal/mol higher in energy.[12] [b] The CASSCF/6-31G* optimized geometry is 0.1 kcal/mol lower in energy. [c] At the CASSCF/6-31G* optimized D_{8h} geometry for the singlet, the lowest triplet lies 15.8 kcal/mol higher in energy.[12]

The D_{4h} transition state was found to connect two D_{2d} minima. As shown in Table I, the barrier to ring inversion via the D_{4h} transition state is computed to be 13.2 kcal/mol at the CASSCF/3-21G level, which increases by 0.6 kcal/mol when corrected for the difference in the two zero-point energies. The CASSCF/3-21G barrier to ring inversion of about 14 kcal/mol[11] is somewhat larger than the barrier of approximately 10 kcal/mol in unsubstituted COT that would be inferred from experiments.[2,3] However, also as shown in Table I, recalculation of the CASSCF energies at the 3-21G optimized geometries with the 6-31G* basis set gave a CASSCF/6-31G* barrier height of 10.0 kcal/mol (10.6 kcal/mol after correction for zero-point energy differences), which is in excellent agreement with experiment.

For the D_{8h} geometry the CASSCF/3-21G vibrational analysis found the single imaginary mode (1962*i* cm^{-1}) to have B_{1g} symmetry and to shorten and lengthen alternate C–C bonds. The E_{2u}, out-of-plane mode was computed to be the vibration of lowest frequency (152 cm^{-1}) at the D_{8h} transition state. However, starting from either the CASSCF/3-21G or 6-31G* optimized D_{8h} geometry, upon small E_u distortions toward a flattened D_{2d} saddle-shaped structure, the CASSCF energy was found to increase quadratically and by nearly the same amount with both basis sets. Larger E_u distortions were also investigated, but our calculations failed to locate a saddle-shaped, D_{2d} stationary point that could serve as an alternate to the planar, D_{8h} geometry as the transition state for bond shifting in COT.

In order to calculate the energy required for bond shifting in planar COT, we compared the energies of the D_{8h}[12] and D_{4h} geometries. The CASSCF energy difference amounts to 5.1 kcal/mol with 3-21G and 6.4 kcal/mol with 6-31G*. However, because the in-plane vibrational modes of D_{4h} COT that involve the localized double bonds are calculated to be of considerably higher frequency than the corresponding modes for the delocalized double bonds of D_{8h} COT, correction for the difference in zero-point energies is significant, amounting to 2.3 kcal/mol. After this correction, the CASSCF energy differences of 2.8 kcal/mol (3-21G) and 4.1 kcal/mol (6-31G*) between D_{8h} and D_{4h} geometries are in excellent agreement with the measured differences of 3–4 kcal/mol between the energies required for bond shifting and ring inversion in monosubstituted derivatives of COT.[3]

The excellent agreement found between the relative CASSCF/6-31G* energies of the D_{2d}, D_{4h}, and D_{8h} stationary points and the experimental barriers to ring inversion and bond shifting in COT provides independent support for our finding that planar geometries of, respectively, D_{4h} and D_{8h} symmetry are the

---

(5) Paquette, L. A.; Trova, M. P.; Luo, J.; Clough, A. E.; Anderson, L. B. *J. Am. Chem. Soc.* **1990**, *112*, 228. Paquette, L. A.; Wang, T.-Z.; Luo, J.; Cottrell, C. E.; Clough, A. E.; Anderson, L. B. *J. Am. Chem. Soc.* **1990**, *112*, 239 and references cited therein.

(6) Ermer, O.; Klärner, F.-G.; Wette, M. *J. Am. Chem. Soc.* **1986**, *108*, 4908.

(7) Binkley, J. S.; Pople, J. A.; Hehre, W. J. *J. Am. Chem. Soc.* **1980**, *102*, 939.

(8) Hariharan, P. C.; Pople, J. A. *Theor. Chim. Acta* **1973**, *28*, 213.

(9) Optimized geometries are available as supplementary material.

(10) CASSCF calculations and numerical vibrational analyses were performed using GAMESS: Dupuis, M.; Spangler, D.; Wedolowski, J. J.; modified by Schmidt, M. W.; Baldridge, K. K.; Boatz, J. A.; Jensen, J. H.; Koseki, S.; Gordon, M. S.; Nguyen, K. A.; Windus, T. L.; Elbert, S. T. *QCPE Bull.* **1990**, *10*, 52.

(11) For previous calculations of the barrier to ring inversion in COT, see: (a) Dewar, M. J. S.; Harget, A.; Haselbach, E. *J. Am. Chem. Soc.* **1969**, *91*, 7521. (b) Wipff, G.; Wahlgren, U.; Kochanski, E.; Lehn, J. M. *Chem. Phys. Lett.* **1971**, *11*, 350. (c) Allinger, N. L.; Sprague, J. T.; Finder, C. *Tetrahedron* **1973**, *29*, 2519. (d) Dewar, M. J. S.; Merz, K. M. *J. Phys. Chem.* **1985**, *89*, 4739. (e) Trindle, C.; Wolfskill, T. *J. Org. Chem.* **1991**, *56*, 5426.

(12) The CASSCF energy of the lowest triplet state ($^3A_{2u}$), which has its minimum at essentially the same D_{8h} geometry as the lowest singlet ($^1B_{1g}$), is higher in energy than $^1B_{1g}$. Thus, as expected from qualitative theory[13] and from the results of previous semiempirical calculations,[11d] D_{8h} COT, like D_{4h} cyclobutadiene,[13] violates Hund's rule.

(13) Review: Borden, W. T. In *Diradicals*; Borden, W. T., Ed.; Wiley: New York, 1982; pp 1–72.

transition states for these processes in COT.[14]

Acknowledgment. We thank the National Science Foundation for support of this research and for a grant that allowed purchase of the Convex C-210 Computer, on which some of these calculations were performed. We also thank the San Diego Supercomputer Center for a generous allocation of computer time.

Supplementary Material Available: Optimized CASSCF/3-21G geometries for D_{2d} and D_{4h} COT and optimized CASSCF/3-21G and 6-31G* geometries for D_{8h} (1 page). Ordering information is given on any current masthead page.

---

(14) Our calculations do not, of course, exclude the possibility of nonplanar transition state geometries in annulated derivatives of COT.[5]

A New Phenol Synthesis from the Rhodium(I)-Catalyzed Reaction of Cyclopropenes and Alkynes[†]

Albert Padwa* and Simon L. Xu

Department of Chemistry, Emory University
Atlanta, Georgia 30322

Received March 20, 1992

The Fischer carbene carbonylation reaction represents an important method for the preparation of a variety of substituted phenols.[1-7] This protocol, as illustrated by the assembly in Figure 1, requires a stoichiometric amount of the metal and works best when the carbene complex is stabilized by an oxygen substituent. We recently initiated a study of the rhodium metal mediated cyclizations of acetylenic diazo ketones.[8a] Such substrates are appealing as synthetic intermediates in that they are readily accessible, are reasonably robust, and produce vinyl carbenoids that are useful for further synthetic transformations.[9,10] We have now explored the potential of these rhodium vinyl carbenoid intermediates to undergo alkyne insertion so as to produce substituted phenols. This approach to phenols nicely complements the more traditional benzannulation reaction of Fischer carbene complexes (i.e., **2** vs **5**).

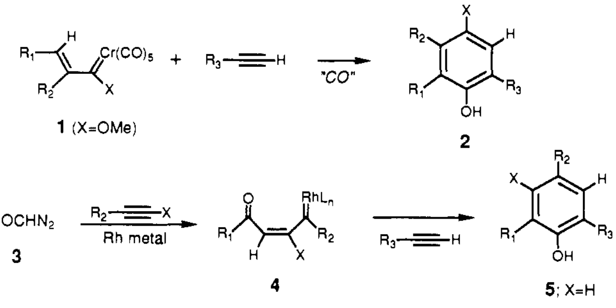

Figure 1. Fischer carbene vs rhodium carbenoid approach to substituted phenols.

Scheme I

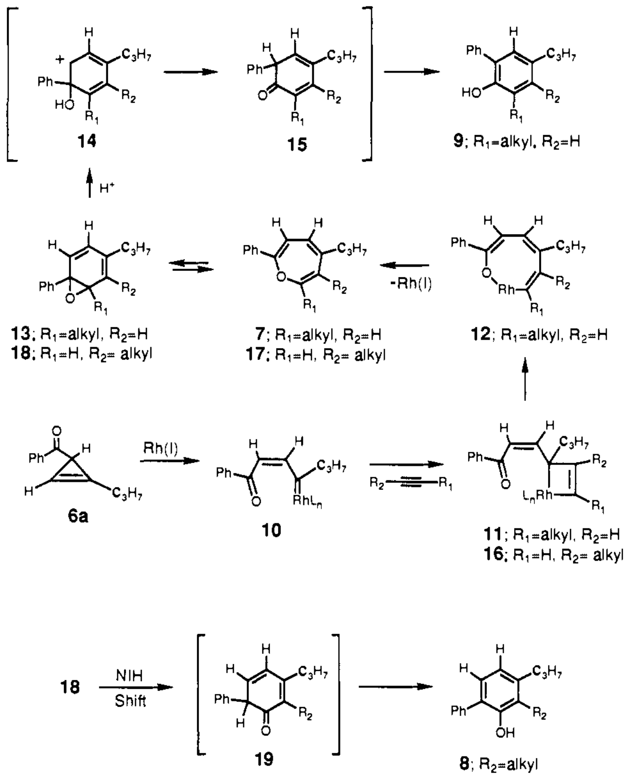

The precursors for the rhodium vinyl carbenoids were prepared in good yields by treating α-diazo benzoyl ketone with various terminal alkynes.[11] The resulting cyclopropene **6** was allowed to stir in methylene chloride with 10 mol % of tetracarbonyldichlorodirhodium in the presence of another terminal alkyne. In a typical reaction, cyclopropene **6a** was reacted with 1-hexyne to give oxepin **7a** (62%) as well as phenol **8a** (8%). A related set of reactions occurred with methyl propargyl ether (**7b** (54%) and **8b** (7%)) as well as with 4-phenyl-1-butyne (**7c** (45%)). The NMR spectrum of oxepin **7a** shows a vinyl singlet at δ 5.45 and two sets of vinylic doublets at 6.05 and 6.27 with a vicinal coupling constant of 6.1 Hz. Treatment of oxepin **7** with a drop of HCl at 40 °C induced a near-quantitative rearrangement to phenol **9**.[12]

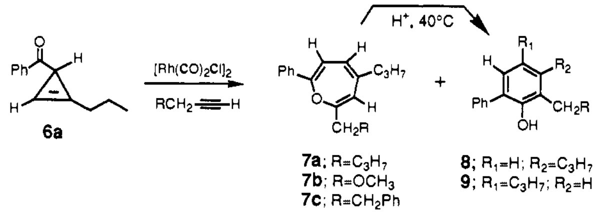

[†] Dedicated to my good friend Al Meyers on the occasion of his 60th birthday.

(1) Dötz, K. H. *Angew. Chem., Int. Ed. Engl.* **1975**, *14*, 644.

(2) For a review, see: Wulff, W. D. In *Comprehensive Organic Synthesis*; Trost, B. M., Fleming, I., Eds.; Pergamon Press: New York, 1990; Vol. 5. Wulff, W. D. In *Advances in Metal-Organic Chemistry*; Liebeskind, L. S., Ed.; JAI Press, Inc.: Greenwich, CT, 1989; Vol. 1. McCallum, J. S.; Kunng, F.-A.; Gilbertson, S. R.; Wulff, W. D. *Organometallics* **1988**, *7*, 2346. Wulff, W. D.; Xu, Y.-C. *Tetrahedron Lett.* **1988**, 415.

(3) Boger, D. L.; Jacobson, I. C. *J. Org. Chem.* **1990**, *55*, 1919.

(4) Yamashita, A. *J. Am. Chem. Soc.* **1988**, *107*, 5823.

(5) Peterson, G. A.; Kunng, F.-A.; McCallum, J. S.; Wulff, W. D. *Tetrahedron Lett.* **1987**, 1381.

(6) Dötz, K. H.; Popall, M. *Tetrahedron* **1985**, *41*, 5797. Dötz, K. H.; Dietz, R. *Chem. Ber.* **1978**, *111*, 2517.

(7) Semmelhack, M. F.; Bozell, J. J.; Keller, L.; Sato, T.; Spiess, E. J.; Wu, W.; Zask, A. *Tetrahedron* **1985**, *41*, 5803.

(8) (a) Padwa, A.; Kassir, J. M.; Xu, S. L. *J. Org. Chem.* **1991**, *56*, 6971. (b) Electrophilic attack of Rh(I) probably occurs initially on the less substituted carbon of the cyclopropene π-bond but the resulting metalated species is equilibrated to the more stable rhodium-carbene complex **10**.[8a,13]

(9) Padwa, A.; Austin, D. J.; Xu, S. L. *J. Org. Chem.* **1992**, *57*, 1330. Padwa, A.; Krumpe, K. E.; Zhi, L. *Tetrahedron Lett.* **1989**, 2623. Padwa, A.; Chiacchio, U.; Gareau, Y.; Kassir, J. M.; Krumpe, K. E.; Schoffstall, A. M. *J. Org. Chem.* **1990**, *55*, 414. Padwa, A.; Krumpe, K. E.; Gareau, Y.; Chiacchio, U. *J. Org. Chem.* **1991**, *56*, 2523. Padwa, A.; Austin, D. J.; Xu, S. L. *Tetrahedron Lett.* **1991**, 4103. Kinder, F. R.; Padwa, A. *Tetrahedron Lett.* **1990**, 6835.

(10) Hoye, T. R.; Dinsmore, C. J.; Johnson, D. S.; Korkowski, P. F. *J. Org. Chem.* **1990**, *55*, 4518. Hoye, T. R.; Dinsmore, C. J. *J. Am. Chem. Soc.* **1991**, *113*, 43. Hoye, T. R.; Dinsmore, C. J. *Tetrahedron Lett.* **1991**, 3755.

(11) Müller, P.; Pautex, N.; Doyle, M. P.; Bagheri, V. *Helv. Chim. Acta* **1991**, *73*, 1233.

(12) The NMR spectrum of **9** showed the aromatic protons to be coupled by 1.5 Hz (meta). In contrast, phenol **8** exhibited a vicinal coupling of 7.5 Hz for the ortho hydrogens.

0002-7863/92/1514-5881$03.00/0